韓國海洋工學會誌 第13卷 第3(Ⅰ)號, pp.114~122, 1999. 8

◉ 論 文

Computation of Free Surface Flows and Detection of Sub - Breaking

Seung-Hyun Kwag*

(99년 3월 2일 접수)

자유표면파 계산 및 준쇄파 수치연구

곽 승 현*

Key Words : Sub-Breaking(준쇄파), Free-Surface(자유표면), Navier-Stokes(나비에스토크스), NACA0012(날개단면), Third Derivative Upwind(3차풍상미분)

초 록

준쇄파(쇄파발생전 리플형태의 불안정파)를 수치적으로 해석하고 예측하기 위하여 수중날개를 대상으로 점성유동장의 계산을 수행하였다. Navier-Stokes 방정식을 사용하여 자유수면을 계산하였고 정도향상을 위하여 Euler 형태의 자유표면조건에 고차의 유한차분법을 적용하였다. 이산화 과정에서 자유표면 격자에 3차 풍상미분항을 적용시켜 수치계산을 수행하였고, 계산결과를 사용하여 준쇄파의 생성조건을 규명하였다.

1. Introduction

Free surface handling and wave-body interaction constitute the most important problems in the submerged hydrofoils moving at a constant speed beneath the free surface. Recently some works have been directed to the solution of Navier-Stokes equations accounting for the presence of a free-surface. Numerical methods for treating such flow problems have been established, but their applications to the free surface have been relatively few. Field discretization methods are most commonly used to solve the Navier-Stokes equations, e.g., the MAC (Marker and Cell) method of Harlow and Welch[1] and its various improved versions such as Nichols & Hirt[2] and Miyata[3]. A review of this subject may be found in Floryan[4]. Field discretization methods have some inherent limitations. With any workable numerical scheme, 'numerical viscosity' is also present. This introduces a numerical diffusion phenomenon

* 종신회원, 한라대학교 조선공학과

in addition to the physical diffusion and gives incorrect solutions for large Reynolds numbers. It is still beyond modern computational capabilities to use so small a grid size that numerical viscosity effects can be reduced to satisfactory levels at realistic Reynolds numbers.

A Lagrangian method was introduced by Chorin[5] which is free of the difficulty of numerical viscosity. Although the MAC method is widely used at present, it only calculates the free-surface elevation in a Lagrangian manner by dislocating the particle according to the local velocity. This is a first order approximation in which no special considerations on the characteristics of waves are made. Moreover, the scheme tends to become unstable after a large number of time steps. In this paper, the third-derivative term is artificially added for the free surface, which is an extension work of Fujita[6], Lungu and Mori[7]. As an application of the present results, the appearance of sub-breaking waves is numerically detected. The criterion for the sub-breaking is applied to the computed results.

2. Numerical Scheme

2.1 Computational Strategy and Boundary Conditions

The Navier-Stokes and continuity equations are governing equations. Details on the basic equations and their relations are referred in the previous paper[8].

The calculation proceeds through a sequence of loops each advancing the entire flow configuration through sufficiently small finite time increments $\triangle t$. The output of each loop is taken as an initial condition for the next one and the computation is performed until T_{max}. An Euler explicit time stepping scheme is used for the time marching procedure. Pressures are obtained throughout the fluid domain by solving the Poisson equation. Iterations are stopped when the pressure difference between two consecutive approximations is smaller than a certain quantity, chosen as a priority. The new pressure field generates a new velocity field. The velocity component updating is achieved by using the time-forward difference form of momentum equations. At the upstream boundary, the flow starts from zero and is accelerated up to the predefined speed. Thus, each horizontal component of velocity has the same constant value depending on the time step. The vertical component is equal to zero in each point of the upstream boundary and remains the same during the pressure computation. The pressure is the static one and remains the same, too. The bottom boundary is located far enough from the still water level. That means the wavy motion influence is so gentle that the zero gradient extrapolation can be used for both components of velocity there. The pressure is set constant at the static value. On the body surface, the no-slip condition for the velocity and the Neumann condition for the pressure are used. The treatment of the free surface is explicitly presented in the following section.

2.2 Free-Surface Boundary Condition

The fluid particle is moved by

$$\frac{\partial h}{\partial t} + u\frac{\partial h}{\partial x} - w = 0 \Big|_{z=\zeta} \qquad (1)$$

The boundary condition for the free-surface requires zero tangential stress and a normal stress that balances any externally applied normal stress. To apply this condition means to know not only the location of the free-surface at each grid point but also its slope and curvature. The tangential stress can be considered zero as a small negligible quantity without influencing

the accuracy of computation as proved by Hinatsu[9]. According to the MAC method, the fluid particle movement is computed by means of the new x and z coordinates and velocities determined at the previous time step. The displacement of the particle is given by

$$\triangle x = u \cdot \triangle t \quad , \quad \triangle h = w \cdot \triangle t \tag{2}$$

where $\triangle t$ is the time increment. The relation is of the first order of approximation for both x and h. The use of (2) to determine the new location of the particle on the free-surface means to define the position locally, not taking into account the influence of the neighbouring particle movements that can accelerate the wave development. On the other hand, the use of an Euler-type expression of the kinematic free-surface boundary condition makes possible to employ a higher finite difference scheme. The condition can be written as follows:

$$\frac{\partial h_i^{n+1}}{\partial t} + (u_i + \frac{\partial u_i}{\partial z} \triangle h_i) \cdot \frac{\partial h_i^{n+1}}{\partial x} - w_i = 0 \tag{3}$$

where $h = h(x, t)$ represents the elevation.

Expanding in Taylor series the function $h = h(t)$ at the $(n+1)^{th}$ and n^{th} time steps, by substraction, the following expression can be obtained:

$$\frac{\partial h_i^{n+1}}{\partial t} = \frac{1}{2\triangle t} \cdot (h^{n-1} - 4h^n + 3h^{n+1}) \tag{4}$$

For the $\partial h^{n+1}/\partial x$ derivative, the third order upwind difference(TOUD hereafter) is one of the most commonly used. As it is already well-known, the TOUD scheme given by:

$$c\frac{\partial h}{\partial x} = c\frac{1}{6\triangle x}(-2h_{i-3} + 9h_{i-2} - 18h_{i-1} + 11h_i) \tag{5}$$

where c is the convective velocity, can be decomposed into two parts. One is the central differencing term whose mathematical expression can be obtained by suitable Taylor expansions of $h = h(x)$ around the point $i-1\frac{1}{2}$ as follows:

$$\frac{c}{24\triangle x}(h_{i-3} - 27h_{i-2} + 27h_{i-1} - h_i) \tag{6}$$

The other is the diffusion term, which has the meaning of the fourth derivative of the velocity.

$$\frac{3c}{8\triangle x}(-h_{i-3} + 7h_{i-2} - 11h_{i-1} + 5h_i) \tag{7}$$

The latter is expected to play a role to compensate the "finiteness" of the differentiation without phase shift. Here we similarly introduce the third derivative, which contributes the phase shift without damping and is also obtained by the Taylor expansions around the point $i-1\frac{1}{2}$ and given as follows:

$$\frac{\alpha c}{(\triangle x)^3}(-h_{i-3} + 3h_{i-2} - 3h_{i-1} + h_i) \tag{8}$$

where $\alpha = -\frac{(\triangle x)^2}{6}$ is a constant.

(8) is added to the right hand side term of (5), and the new formulation for the $\partial h/\partial x$ that will be used in the free-surface definition can be written:

$$c\frac{\partial h}{\partial x} = c\frac{1}{6\triangle x}(-h_{i-3} + 6h_{i-2} - 15h_{i-1} + 10h_i) \tag{9}$$

(9) is the same expression used by Dawson[10] in his steady flow problem by using the Rankine source method where he derived $\partial h/\partial x$ omitting the terms of the third derivative intuitively.

Introducing (4) and (9) into (3) and referring the relation of $\triangle h^n_{i-1} = h^{n+1}_{i-1} - h^n_{i-1}$ and

$\frac{\partial h^{n+1}}{\partial x} = \frac{\partial h^n}{\partial x} + \frac{\partial \triangle h^n}{\partial x}$, the vertical coordinate increment at each time step can be found:

$$\triangle h_i^n = \frac{3\triangle x(h_i^n - h_i^{n-1}) + \triangle t \cdot [6w_i \triangle x + u_i(\triangle h_{i-3}^n - 6\triangle h_{i-2}^n + 15\triangle h_{i-1}^n - Q_i^n)]}{9\triangle x + \triangle t \cdot [10u_i + Q_i^n \frac{\partial u}{\partial z} - 6\triangle x \frac{\partial w}{\partial z}]} \quad (10)$$

The expression is of the second order accuracy for $h(0(h^2))$ for any $u>0$. $Q^n{}_i$ in (10) is

$$Q_i^n = -h_{i-3}^n + 6h_{i-2}^n - 15h_{i-1}^n + 10h_i^n \quad (11)$$

Finally, h at the $(n+1)^{th}$ time step is calculated by:

$$h^{n+1} = h^n + \triangle h^n \quad (12)$$

Besides, the same discretization of spatial derivatives for the governing equations is made. A quadri-diagonal system of equations is obtained and solved in the same manner as those for velocity and pressure. On the free-surface, the exact pressure condition is imposed because the uppermost grid is always identical to the water surface. By this scheme, it is expected that the free-surface condition(i.e., the constant pressure condition) can be directly applied without any interpolation.

2.3 Numerical Wave Absorber

On the open boundary, since the exact condition is quite difficult to express, pressures and velocities are usually extrapolated with zero gradient from those values found inside the domain. A doubt should be thrown if such a treatment is valid for a free-surface flow case where pressures and velocities are periodically fluctuating. In the present work, a suppression of the vertical component of velocity for a certain range in x-direction is imposed as a downstream boundary condition. This is equivalent to a wave absorber, which is expected to reduce the reflection from the downstream boundary. The flow along the absorber is similar to that through parallel plates where the friction between the particle and plate modifies the velocity field.

There is much concern as to the proper model to employ. Therefore several mathematical formulation are attempted for the numerical absorber as follows.

$$w^n(i,k) = \frac{x(i_m,k) - x(i,k)}{x(i_m,k) - x(i_m - i_a,k)} \cdot w^n(i_m - i_a,k) \quad (13)$$

$$w^n(i,k) = \left[\frac{x(i_m,k) - x(i,k)}{x(i_m,k) - x(i_m - i_a,k)}\right]^2 \cdot w^{n-1}(i,k) \quad (14)$$

where

$$i \in [i_m - i_a, i_m], \quad k \in [1, k_{max}]$$

Solutions obtained by using (13) and (14) proved that the strong decrease of w may generate a rather strong modification of both pressure and velocity fields at the far downstream. Better results are obtained by using a smoother suppression of the vertical component of velocity. In this case the mathematical model is as follows:

$$w^n(i,k) = \frac{-w^n(i_m - i_a,k) \cdot [x(i_m - i_a,k) - x(i,k)]^2}{2 \cdot [x(i_m - \frac{i_a}{2},k) - x(i_m - i_a,k)]^2} + w^n(i_m - i_a,k) \quad (15)$$

$$\text{if} \quad i_m - i_a \le i \le \frac{i_m - i_a}{2},$$

$$w^n(i,k) = \frac{w^n(i_m - i_a,k) \cdot [x(i,k) - x(i_m,k)]^2}{2 \cdot [x(i_m - \frac{i_a}{2},k_m) - x(i_m,k_m)]^2} \quad (16)$$

$$\text{if} \quad \frac{i_m - i_a}{2} \le i \le i_m$$

where i_m and k_m represent the total number of the grid lines in the horizontal and vertical directions respectively. The superscripts denote the time step. i_a denotes the number of the first grid cell of the absorber. The modification is carried out at every time step.

3. Results And Discussion

3.1 Computational Conditions:

The hydrofoil shape of NACA0012 is used at 30° angle of attack. The submergence depth is 1.592 times the chord length. The computing domain is 7 times as large as the chord in the streamwise direction. The minimum grid spacing in z direction is 0.002. The oncoming flow has been accelerated from 0 to 0.5 from the beginning. Four computations are carried out to compare with the experimental results. The grid is made as H-H topology to treat the free-surface movement more conveniently, but relatively a large number of iterations are requested near the leading edge. Fig. 1 shows the coordinate system and grid view for the computation.

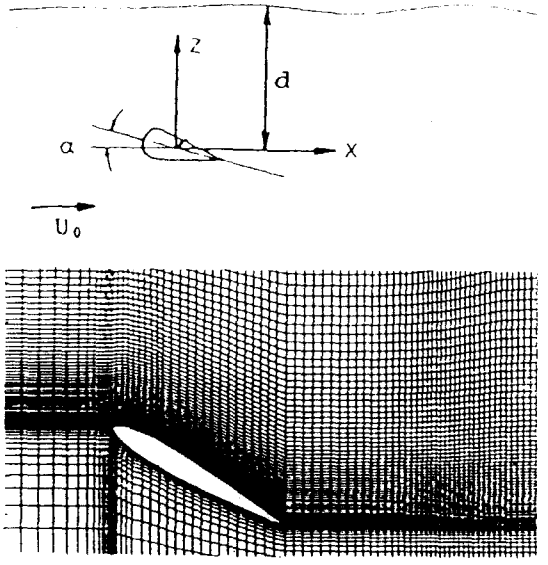

Fig. 1 Coordinate system and grid

3.2 Computational Results

The free-surface wave profiles are shown in Fig. 2. It presents a comparison between the computation and experiment. The free-surface wave has been developed by using the new finite difference scheme of the Euler-type formulation. It is a result of the third derivative introduced in the numerical simulation. Fig. 3 shows the velocity vectors around the hydrofoil at four different speeds. Fig. 4 shows the computed pressure contours, which strongly depends on the Froude number as expected.

3.3 Application to Detection of Sub-breaking Waves

As an application, sub-breaking waves are numerically detected in the free surface flows around the submerged hydrofoil. The sub-breaking waves are ripple-like waves which are supposed to be caused by the instability of the free surface flow. An instability analysis[11] provides a critical condition for their appearance.

$$\frac{M}{U}\frac{\delta M}{h\delta s}-\frac{\delta U}{h\delta s}-\frac{1}{n_z}\frac{\delta n_z}{h\delta s}>0 \tag{16}$$

where

$$M=(\kappa U^2-n_z\cdot g)\cdot n_z \tag{17}$$

s is the streamline coordinate along the free surface and h is its metric coefficient, while n is the normal; n_z the direction cosine of n to z. U_o is the velocity component of the basic flow in the s-direction; κ is the curvature of the free surface and g the gravity acceleration. Limiting ourselves to a narrow proximity to the wave crest, we assume $n_z \fallingdotseq 1$ and $\delta/h\delta s \fallingdotseq \delta/\delta x$, then (16) can be reduced approximately to

$$\frac{U^2}{M}\frac{\delta}{\delta x}\frac{M}{U}>0 \tag{18}$$

where

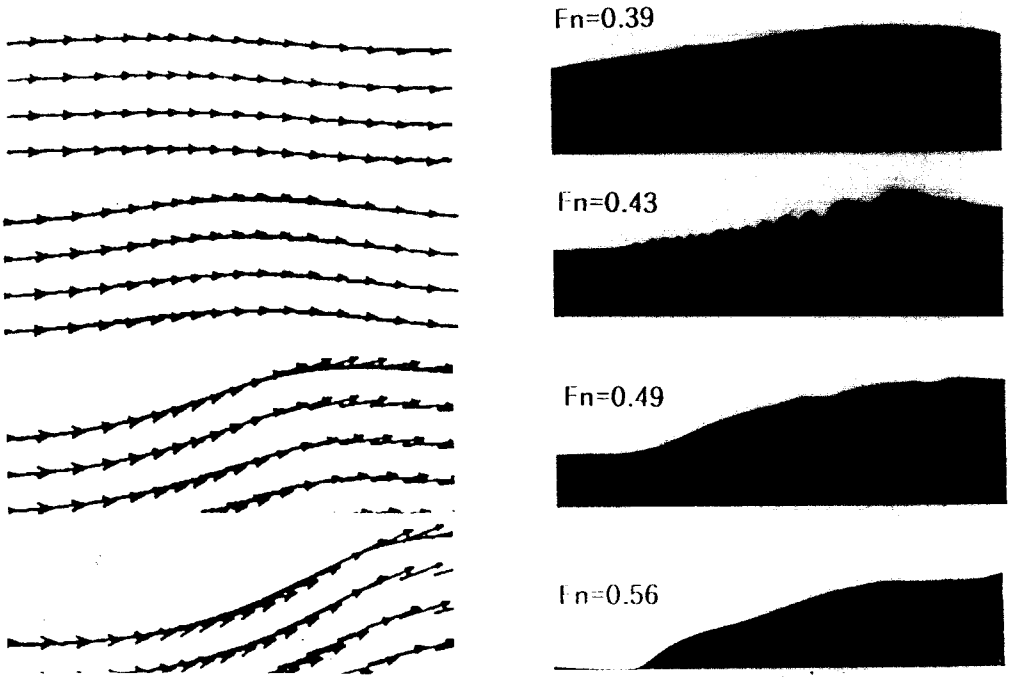

Fig. 2 Free-surface distortion as a function of Froude number based on chord of hydrofoil. Actual length is 90% of chord. (lhs:computation, rhs:experiment[12])

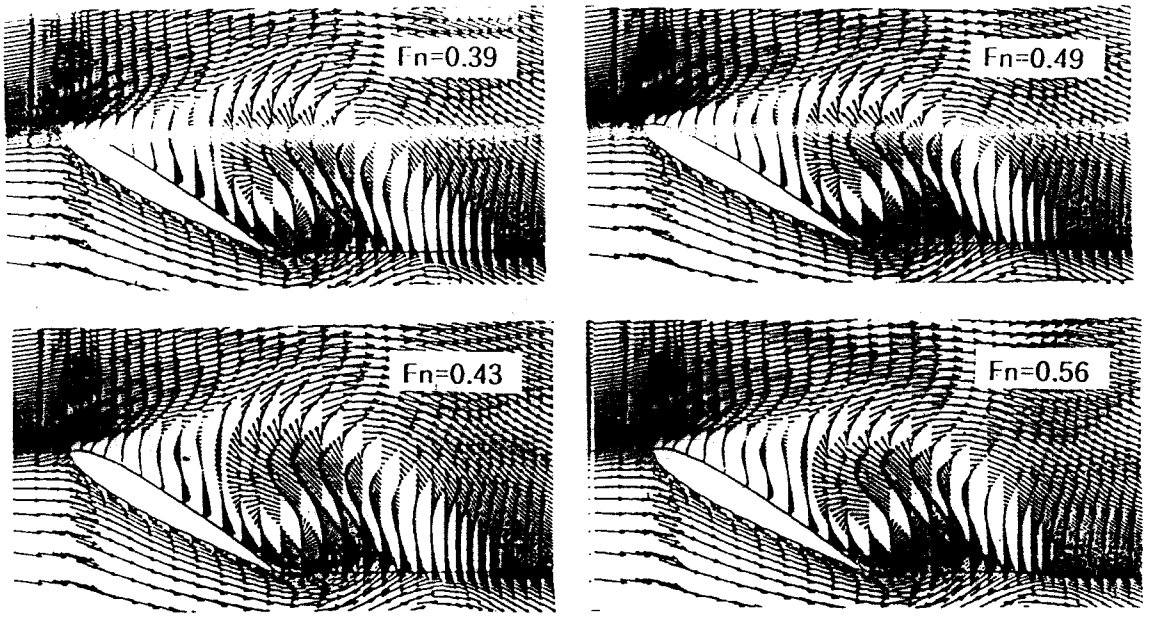

Fig. 3 Velocity vectors around hydrofoil as a function of Froude number (Fn=0.39, 0.43, 0.49, 0.56)

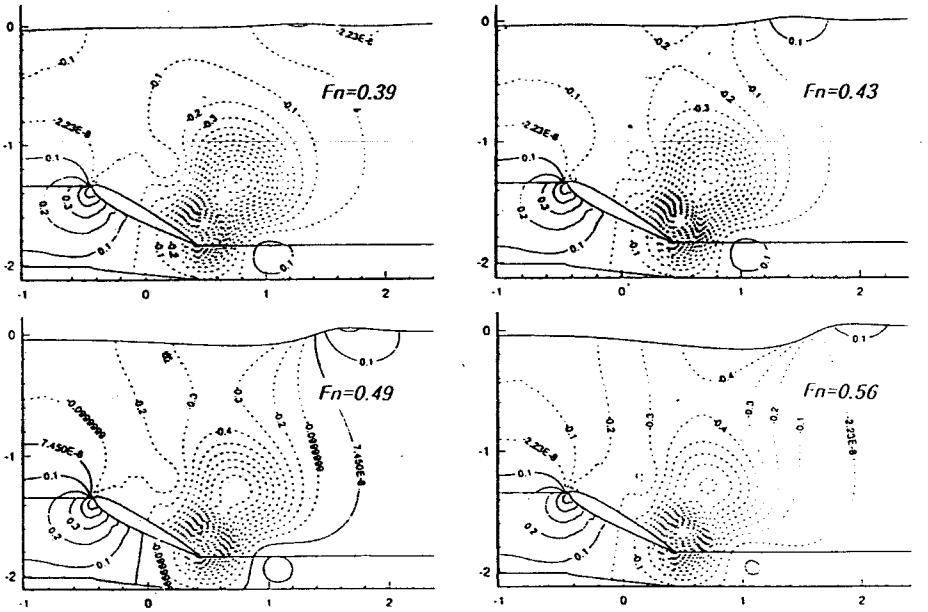

Fig. 4 Pressure contours around hydrofoil as a function of Froude number (Fn=0.39, 0.43, 0.49, 0.56)

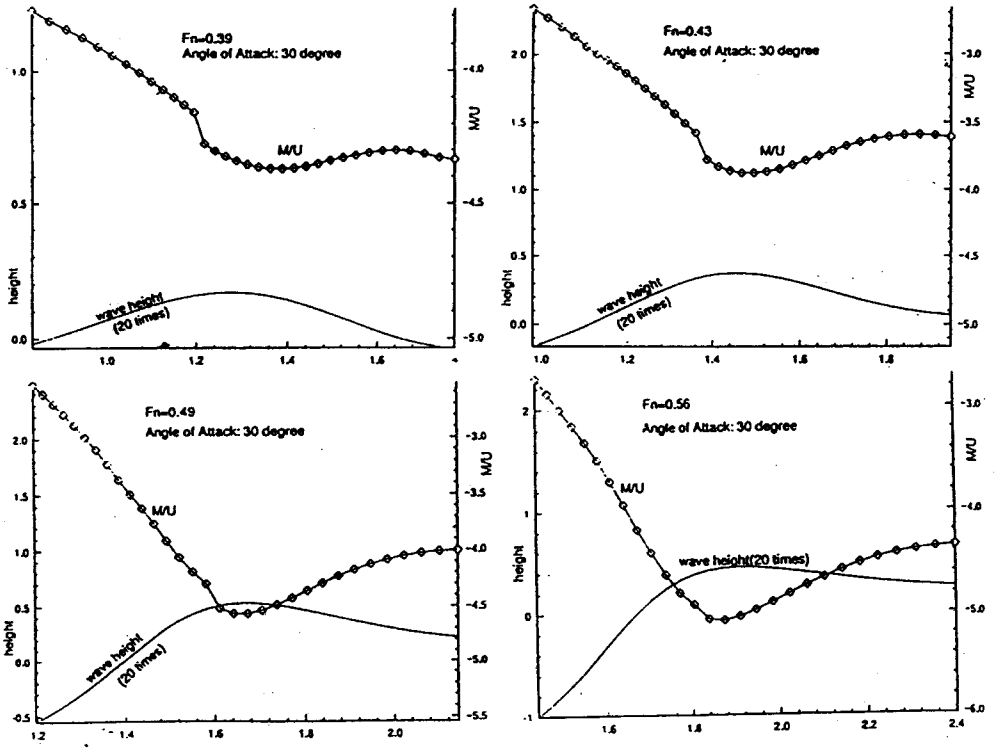

Fig. 5 Variations of M/*U* and free-surface elevation

$$M = \kappa U_o^2 - g \qquad (19)$$

Fig. 5 shows the variations of M/U vs. x around the first wave crest. The analysis is made along the curved waves and those at four speeds of Fn=0.39, 0.43, 0.49 and 0.56 are compared. Because M is negative, the negative gradient of M/U to x suggests the possibility for the free surface flow to be unstable. Steep negative gradient can be seen as the speed increases.

4. Conclusion

1) The free-surface boundary condition with the third derivative gives the good results in the simulation of viscous flows around the hydrofoil. The wave in the far downstream can be made by using the numerical wave absorber.

2) The free-surface wave can be generated at the large angle of attack 30° which usually gives some numerical trouble, divergence. It means that the present scheme can treat free-surface flows more efficiently with the new finite difference scheme.

3) It is numerically confirmed that the criterion for the appearance of sub-breaking waves works qualitatively, and the present scheme can be applied to detect the occurrence of breaking waves.

References

1) Harlow, F.H. and J.E. Welch, "Numerical Calculation of Time-Dependent Viscous Incomp- Ressible Flow of Fluid with Free Surface", Phys. Fluids, Vol. 8, pp.2182~2189, 1965

2) Nichols, B.D. and C. W. Hirt, "Improved Free-Surface Boundary Conditions for Numerical Incompressible Flows", J. Comp. Phys., Vol. 8, pp.434~448, 1971

3) Miyata, H., "Finite-Difference Simulation of Breaking Waves", J. Comp. Phys., Vol. 65, pp. 179~214, 1986

4) Floryan, J.M. and H. Rasmussen, "Numerical Methods for Viscous Flow with Moving Boundaries", Applied Mech. Rev., Vol. 42, pp. 323~341, 1989

5) Chorin, A. J., "Numerical Study of Slightly Viscous Flow", J. Fluid Mech., Vol. 57, pp.785~796, 1973

6) Fujita, K., "On More Accurate and Efficient Methods for the Free-Surface Flow Computation by the Finite Difference Method", Master Thesis, Hiroshima University, in Japanese), 1992

7) Lungu, A., K. Mori, "A Study on Numerical Schemes for More Accurate and Efficient Computation of Free-Surface Flows by Finite Difference Method", Jour of the Soc of Naval Arch of Japan, Vol. 173, pp.9~17, 1993

8) Kwag, S.H., K.S. Min, "Computation of Free Surface Flows Around 3-D Hydrofoil and Wigley Ship by N-S Solver", 6th Int Conf on Numerical Hydro, Iowa, pp.271~288, 1993

9) Hinatsu, M., "Numerical Simulation of Unsteady Viscous Nonlinear Waves Using Moving Grid System Fitted on a Free Surface", J. of Kansai Society of Naval Arch., Japan, Vol. 217, pp.1~11, 1992

10) Dawson, C.W., "A Practical Computer Method for Solving Ship-wave Problems", Proc. of 2nd Int. Conf. on Numerical Ship Hydro-Synamics, Univ. of California, Berkeley, pp.30~38, 1977

11) Mori, K., M. Shin, "Sub-Breaking Wave: Its Characteristics, Appearing Condition and Numerical Simulation", Proc. 17th Symp on Naval Hydro, ONR Research, 1988

12) Lin, J.C., D. Rockwell, "Evolution of a Quasi Steady Breaking Wave", J. Fluid Mech., Vol. 302, pp.29~44, 1995

13) 정세민, 이영길, 이승희, 홍성완, "자유표면 아래서 운동하는 수중익주위의 점성유동해석",

대한조선학회논문집, Vol. 32, pp.72~82, 1995
14) 강국진, "수치파도 시뮤레이션 방법에 의한 자유표면 아래의 날개주위 쇄파영역 탐지", Hull Form, pp.184~192, 1996
15) 박종천, Miyata, "쇄파현상을 포함한 3차원 비선형 자유표면 유동의 수치해석", 대한조선학회 추계강연논문집, pp.67~73, 1995
16) 허재경, 이영길, "수치계산법에 의한 해안에서의 쇄파시뮤레이션", 대한조선학회 추계강연논문집, pp.264~267, 1994
17) 신명수, "2차원 수중익 주위의 점성유동장 해석", 박사학위 논문, 1989
18) 반석호, 김형태, "A Computational Study on Turbulent Flow Characteristics around Full-form Tankers", 대한조선학회 영문논문집, Vol. 2, No. 2, pp.1~13, 1996